Int. J. Appl. Math. Comput. Sci., 2002, Vol.12, No.2, 209–219

FUZZY LOGIC GAIN SCHEDULING FOR NON-LINEAR SERVO TRACKING

MIECZYSŁAW A. BRDYŚ*, JONATHAN J. LITTLER*

* School of Electronic, Electrical and Computer Engineering
University of Birmingham, Birmingham B 15 2TT, UK
e-mail: m.brdys@bham.ac.uk

This paper proposes the use of gain scheduling as a method of controlling a servo system with hard non-linear elements. The servo controls two elements of a tracker mounted on a ship at sea. There is stiction at the zero velocity point and non-linear friction against the motion of each tracker axis. A dual feedback loop control structure is employed. Fuzzy logic is used to provide smoothly varying non-linear scheduling functions to map the velocity of the servo relevant to the deck of the ship onto the rate loop controller parameters. Consideration is given to the use of a derivative signal as a secondary input to the fuzzy inference system. Results are presented which demonstrate that this method of controlling the servo system gives a dramatic improvement over the traditional linear control methodology for low velocity tracking performance. A linear PID controller is used in the outer loop and its design is also given some consideration.

Keywords: tracking, servo control, gain scheduling, fuzzy logic, stiction friction, hard non-linearities

1. Introduction

The servo under consideration in this paper is mounted on a ship at sea. The ship is in motion and is also subject to various disturbances such as wind and sea waves. The servo controls two axes of a tracker, namely the elevation axis and the training axis, representing two perpendicular degrees of freedom. The training axis represents the horizontal plane, parallel to the deck of the ship, and the elevation axis represents the vertical plane, perpendicular to the deck of the slop. These axes can be assumed to be mutually independent. This is shown diagrammatically in Fig. 1.

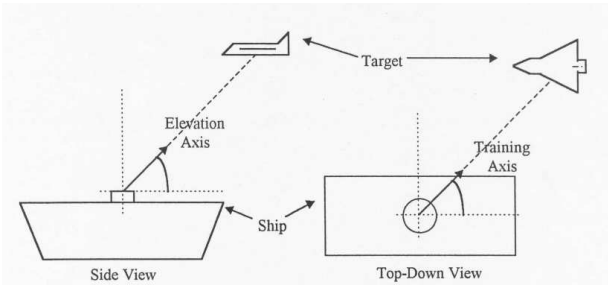

Fig. 1. Overview of the tracking problem.

Traditional methods of controlling the servo system using linear control techniques are inadequate because of hard non-linearities in the dynamics. Stiction at zero velocity creates large transient errors for low velocity tracking operation. Recent papers (Canudas de Wit *et al.*, 1995; Canudas de Wit and Lichinsky, 1997; Lichinsky *et al.*, 1999) consider stationary servo systems described by typically second-order linear dynamics and highly complicated non-linear hard dynamics due to the friction phenomenon. They propose a compensation approach in order to handle the friction. This requires a good friction model that is not available so that the friction model parameters are estimated on-line leading to complicated adaptive control algorithms. Gain scheduling is a well established control technology for controlling the non-linear systems (Shamma and Athans, 1990; Hunt and Johansen, 1997). Its application to uncertain systems is still under development. However, fuzzy logic scheduling of controller parameters was found simple and effective in a number of applications (Brdyś and Sim, 1995; Brdyś *et al.*, 1995, Passino and Yurkovich, 1998). This paper utilises a standard dual feedback loop approach to controlling tracking servos (Garnell and East, 1997), and develops a new controller by scheduling the gains of the inner loop controller as a function of the operating point of the system. This refinement allows the non-linear elements of the dynamics to be compensated for in the inner loop. Fuzzy logic is used to realise the scheduling algorithms for the controller parameters because it allows smoothly varying non-linear functions to be created. The design of appropriate scheduling functions is the central aspect of the controller design. The entire system is simulated to compare the performance of the original and gain scheduled inner loop controllers.

The following sections describe the dynamics of the servo tracker, and then describe in detail the control

methodology used and the design of the inner loop controller. The design process for the outer loop controller is also considered. Finally, some results are presented which show the improvements made over the use of fixed linear controllers.

2. Plant Dynamics

The dynamics of the two tracker axes are very similar, with the only difference in the disturbance inputs. The dynamics are highly non-linear, and this is due to friction and stiction in the servo. Mathematically, the dynamics can be represented by the following two equations:

$$J\frac{\mathrm{d}^2\theta}{\mathrm{d}t^2} = T_M - T_W - T_{OB} - T_f \quad \text{if the axis is outside stiction,} \tag{1}$$

$$\frac{\mathrm{d}\theta}{\mathrm{d}t} = v_s \quad \text{if the axis is in stiction,} \tag{2}$$

where θ is the axis angle in spatial co-ordinates, J stands for the inertia moment, T_M signifies the motor torque (control input), T_W denotes the wind torque (disturbance input), T_{OB} is the out-of-balance torque (disturbance input), T_f means the friction torque, and v_s is the ship motion rate relative to the particular axis.

The stiction phenomenon is the dominant non-linearity which greatly complicates the dynamics. When the velocity of the tracker axis falls to zero with respect to the motion of the ship (i.e. the velocity to deck is equal to zero), the servo becomes 'stuck' and its position remains constant with respect to the ship. The servo then remains in this situation until the servo input torque, T_{in}, is greater than a fixed value known as the stiction torque, T_s. At this point the dynamics return to those described by (1). The input torque is the torque provided by the motor T_M minus the disturbance torques T_W and T_{OB}, representing the wind and out-of-balance disturbance torque inputs, respectively:

$$T_{\mathrm{in}} = T_M - T_{OB} - T_W. \tag{3}$$

2.1. Friction Model

Out of stiction, the friction in the plant dynamics can be modelled as comprising two components, namely static friction and dynamic viscous friction. The static friction is constant, but always acts against the motion of the tracker, and the dynamic friction can be modelled as a linear function of the velocity to deck (the velocity of the tracker axis relative to the deck of the ship) outside a certain dead-zone centred on the zero velocity to deck. Graphically this is shown in Fig. 2. T_b is the bias friction level which represents the value of the static friction. The exact coefficients of the friction model depend on the temperature, which can therefore also be viewed as a plant disturbance.

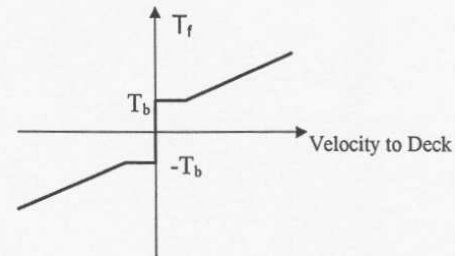

Fig. 2. Friction as a non-linear function of the velocity to deck.

2.2. Plant Disturbances

The ship motion is a disturbance on the output of the servo system, so that the velocity of the tracker relative to the target (the velocity to space, v_s) is composed of the ship motion rate $d(t)$ and the velocity of the tracker relative to the deck of the ship v_d:

$$v_s(t) = d(t) + v_d(t). \tag{4}$$

Assuming that the ship is not under any applied movement, its motion will be entirely due to the 'roll' of the ship. This is caused by sea waves and can therefore be modelled as a sine function with a low frequency and a specific amplitude. The frequency will be the same for both tracker axes, but the amplitude will depend on the specific conditions. It is assumed in this paper that the relative ship motion rates are given by (5) and (6), where the rate of the angular motion is in radians per second. This model assumes that the amplitude of the roll is ten degrees on the elevation axis (i.e. the maximum deviation from the vertical reference position) and five degrees in the training axis.

$$d(t) = 0.11\sin(0.27\pi t) \quad \text{(elevation axis),} \tag{5}$$

$$d(t) = 0.55\sin(0.2\pi t) \quad \text{(training axis).} \tag{6}$$

The other two disturbances effect the input torque to the servo system and can therefore be considered to be plant disturbances. Both are plant state dependent and therefore constitute an important part of the dynamics of the tracker. The first is the wind torque disturbance, the cause of which is self explanatory. The wind torque can be divided into two separate components, known as the static and dynamic wind torques. The static wind torque depends on the angular position and can be modelled as a sinusoidal function of the training axis angle for both axes:

$$T_{W(\mathrm{static})} = W_t\sin(\theta + \phi_t) \quad \text{(training axis),} \tag{7}$$

$$T_{W(\mathrm{static})} = W_e\sin(\theta + \phi_e) \quad \text{(elevation axis),} \tag{8}$$

where W_t and W_e are amplitude constants related to the strength of the wind, ϕ_t and ϕ_e are phase terms for the initial conditions of the training and elevation axes, respectively, and θ is the angular position of the training axis. The values for the amplitudes and phases in expressions (7) and (8) depend on the plant environment at any point in time. The dynamic wind torque is linearly dependent on the angular velocity of the relevant axis, with a dead-zone around the zero velocity point. Graphically, this is shown in Fig. 3. The coefficients representing the linear relation and the width of the dead-zone are dependent on the specific axis and the wind speed.

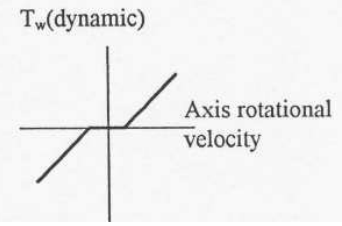

Fig. 3. Dynamic wind torque.

The other torque disturbance is known as the out-of-balance torque, and it arises from gravitational effects. Similarly to the wind torque, the out-of-balance torque can be divided into static and dynamic components. The static component is due to the unbalanced mass that the tracker consists of being off the centre of the axis, and the dynamic component is due to the acceleration of the mounting of the tracker. For the training axis both the out-of-balance torque components are governed by the motion of the slop and so they vary sinusoidally. The maximum disturbance torque will occur when the two components vary in phase, giving a resultant sinusoid:

$$T_{OB} = B_t \sin(\omega t) \quad \text{(training axis)}. \tag{9}$$

The situation is somewhat different on the elevation axis, where the static out-of-balance torque can be taken as constant and the dynamic component varies as before, giving

$$T_{OB} = A + B_e \sin(\omega t) \quad \text{(elevation axis)}. \tag{10}$$

In (9) and (10), B_t and B_e denote the amplitudes while A is a bias.

2.3. Model Validation

Simulation models were developed for both the tracker axes, incorporating all the dynamics already mentioned for a naval case study. The response of the open-loop system to a sinusoidal reference signal was examined. Figure 4 shows the simulated response of both the axes to the following input signals:

$$r(t) = 0.55 \sin(120t)$$

(elevation axis input in radians per second),

$$r(t) = 0.8 \sin(30t)$$

(training axis input in radians per second).

For these tests the disturbance model was not included in the simulation, so that the stiction phenomenon could be observed more clearly. The resulting graphs show the zero crossing behaviour caused by the stiction in the servo and they match well the site test measurements.

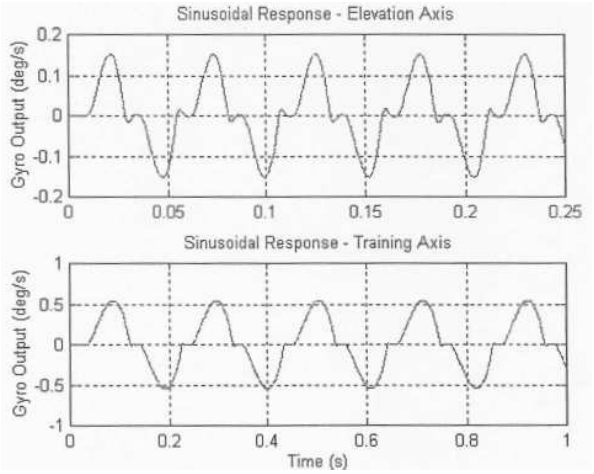

Fig. 4. Open loop sinusoidal responses.

3. Formulation of the Control Problem

3.1. Control Objectives

The highly non-linear nature of the plant (and the stiction phenomenon in particular) means that there are problems operating at velocities close to zero. Significant errors occur when following a reference signal that requires the tracker to change its direction of motion, meaning that the angular rate has to pass through the zero velocity point. Such is the case when the target position remains stationary, meaning that the servo has to move to compensate for the motion rate (or 'roll') of the ship. Since the ship's motion is sinusoidal, the tracker has to periodically change the direction in which it moves relative to the ship's deck in order to maintain the zero motion relative to the target. This results in the system exhibiting a response known as the 'end of roll transient' behaviour, or 'ERT'. It is this situation that causes serious tracking errors and it is therefore the most critical problem that the servo controller deals with. Testing the servo controller with a zero reference

input (or a small step input) to the outer position loop (or the inner velocity loop) is therefore the most important method of evaluating the performance. The specifications are more difficult to reach on the elevation axis, so the controller design focused on this axis. The remainder of this paper refers exclusively to the elevation axis, but the results for the training axis are very similar.

3.2. Control Structure

The basic control scheme for this application uses a traditional solution to servo control problems, incorporating two feedback loops. This is shown schematically in Fig. 5. The inner loop feeds back the velocity signal and the outer loop feeds back the angular position signal. In each loop the relevant error signal is then used as the input to a controller block. The motivation behind this approach is that any errors occurring in the tracking performance are corrected by the velocity loop before they can effect the position tracking response, since the velocity loop is inherently faster than the position loop. This approach also means that the non-linear elements in the system can be compensated for by the inner loop so that the position loop 'sees' only a linear subsystem. The outer loop controller can therefore be used to obtain the required tracking performance. The fact that full state feedback (both position and velocity) is required complicates the control structure. The target position sensors are electro-optical (EO) sensors which introduce a processing delay into the outer loop. The filter before the outer loop controller is therefore designed to compensate for this delay. A Kalman filter is used for this purpose (Singer and Behnke, 1970). The velocity sensor is a gyro which introduces additional dynamics and unwanted sensor noise into the inner loop. The dynamics of the naval tracker gyro were accurately identified as a second-order linear system:

$$G(s) = \frac{1}{1.41 \cdot 10^{-6} s^2 + 1.045 \cdot 10^{-3} s + 1}. \qquad (11)$$

The sensor noise can be modelled as the sum of three components: two sinusoids at frequencies of 268.75 Hz and 400 Hz, and white noise. The amplitudes of the sinewaves are such that they contain 40% of the total noise power. The spectrum of the noise coincides with the desired operating bandwidth of the servo system, and this necessitates the introduction of a filter to clean the measured velocity signal. The design of such a filter is a compromise between the degree of noise rejection required and the detrimental effects of the filter on the speed of the feedback loop. A good compromise was obtained with a second-order Butterworth filter with a cut-off frequency of 160 Hz, having the transfer function

$$H(s) = \frac{1}{9.901 \cdot 10^{-7} s^2 + 1.0 \cdot 10^{-3} s + 1}. \qquad (12)$$

The inner loop also contains an actuator which can be modelled as a combination of a linear gain and nonlinear saturation. The presence of actuator saturation further complicates the system, but only effects the tracking performance at high velocities. The inner control loop is shown in detail in Fig. 6.

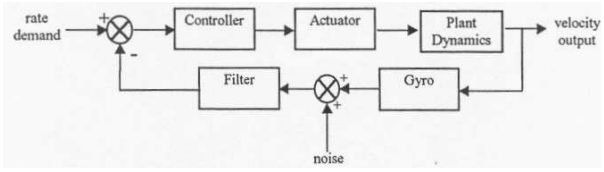

Fig. 6. Inner loop overview.

3.3. Limitations of Fixed Linear Inner Loop Controllers

The simulated response of the servo system to a zero reference input to the outer loop is shown in Fig. 7. The end of roll transient error spikes at the 5 and 10 second instants can clearly be seen. For this simulation a linear PI controller was used in the velocity loop. The controller had the transfer function

$$C(s) = 0.563 \frac{s + 33.3}{s}, \qquad (13)$$

and it represents the optimum fixed linear controller which reduces the transient error as far as possible, but also guarantees the closed loop stability. Similarly, a fixed linear controller was used in the position loop, having the transfer function

$$D(s) = 5 \frac{s + 2}{s}. \qquad (14)$$

For this situation the transient error is greater than the specifications for low velocity tracking which state that the position error should never exceed one minute of a degree.

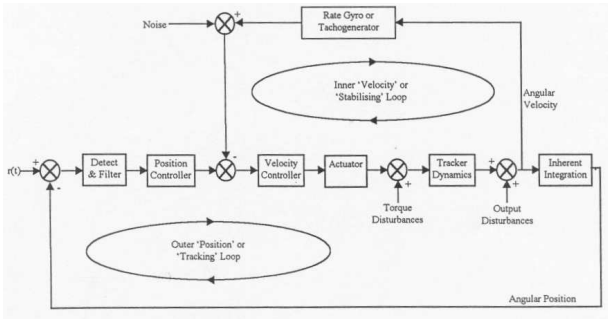

Fig. 5. General control structure.

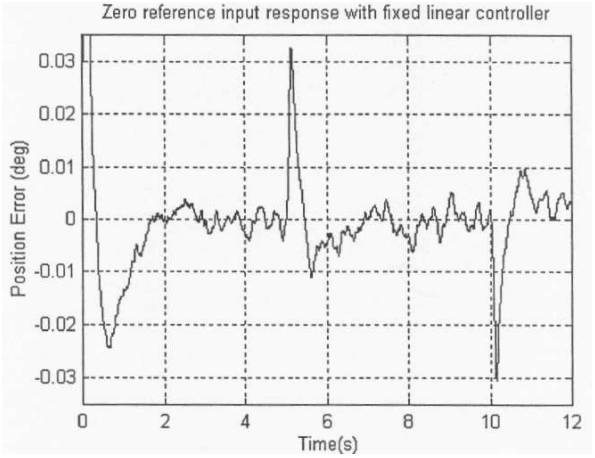

Fig. 7. Best fixed linear controller response.

4. Inner Loop Controller Design

4.1. Control Methodology

The inner loop controller is directly connected with the hard non-linearities in the plant model. It is natural to compensate for the non-linear elements of the plant with an appropriate non-linear controller. The use of a non-linear gain scheduled inner loop controller has been investigated during the course of this work. This control methodology functions by using a PI (proportional plus integral) controller with the constant structure of

$$C(s) = K\frac{s+T_i}{s}, \tag{15}$$

and by varying the parameters K and T_i (the proportional and integral gains) according to the operating point of the system.

This method allows the non-linearities to be compensated for. The dominant problem of stiction can be dealt with by varying the proportional and integral gains as functions of the velocity to deck at any instant in time. At the zero velocity to deck the gains have to be high to ensure that the system is driven out of stiction as soon as possible, minimising the end-of-roll transient error, while out of stiction (with non zero velocity to deck) the controller gains have to be lower so that the sensor noise in the system is not amplified dramatically and so that the closed-loop system robustness is ensured. The design procedure for the controller first required the identification of suitable parameters for the various operating points under consideration, and then the design of suitable scheduling algorithms to interpolate between the different parameter values. A fuzzy inference system can be used to provide a smoothly varying function that maps the value of the velocity to deck onto appropriate controller gain values. Fuzzy logic is a suitable method of mapping input to output because of the ease with which non-linear relations can be realised. This particular application also lends itself to the application of fuzzy supervised control because the situation can be expressed in a simple linguistic manner:

'*When in stiction use high controller gains,*

when out of stiction use lower gains,'

The inner loop control scheme is shown in Fig. 8. The velocity signal is fed back twice, to generate the velocity error signal and also as the input to the fuzzy supervisor. The fuzzy systems used to schedule the proportional term K and the integral controller term T_i can be treated completely separately. The fuzzy supervisor is therefore comprised of two individual inference systems—one mapping the velocity to deck onto a proportional gain and the other mapping the velocity to deck onto an integral gain.

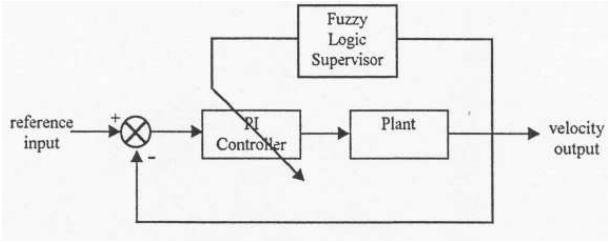

Fig. 8. Control methodology.

4.2. Fuzzy Inference System Design

Proportional Gain Scheduling

Many different fuzzy inference systems were considered in an attempt to reduce the tracking error to a level as low as possible, with different rule bases and input and output membership functions. Initially a fuzzy system with triangular membership functions on the input and output using just two fuzzy rules was used:

1. *If velocity is **ALMOST ZERO** then gain is **HIGH**;*
2. *If velocity is **BIG** then gain is **LOW**.*

It was found that increasing the number of input and output triangular membership functions up to seven generated smoother velocity-gain relations and therefore gave increasingly better performance in terms of reducing the transient error. This motivated the use of 'non-linear' membership functions, since they could provide a smoother relation while only requiring a minimum of fuzzy rules. Using the rule base described above, two different sets of input and output membership functions gave impressive results, and these systems are considered here. The first ('fuzzy inference system 1') used Gaussian piecewise linear 'z'-shaped functions for the input

fuzzy sets, and triangular functions for the output sets. The other inference system ('fuzzy inference system 2') used Gaussian membership functions for both the input and output fuzzy sets. Figures 9–12 show the membership functions used in these fuzzy engines. In these four figures the y-axis represents the grade of membership of the fuzzy sets, and the relevant input sets are labelled 'almost zero' and 'big' while the output sets have the labels 'low' and 'high'. The resulting velocity-to-gain mappings are shown in Fig. 13. Throughout the work, the 'sup-star' compositional rule of inference with 'min' t-norm and with the conjuctive interpretation of fuzzy conditional statement 'if-then' was utilised along with the centre-of-gravity method of defuzzification (Wang, 1994). The choice of this type of the defuzzification process is justified by noting that it produces the smoothest mappings between the input and the output for the fuzzy inference system. Other defuzzification methods (such as the mean of maxima and bisector of area methods) were also used in the fuzzy engines, but were found to produce a more 'stepped' scheduling function, which gave inferior results when simulated as part of the servo control system. This was always likely because the fuzzy systems were designed with the centroid method of defuzzification in mind.

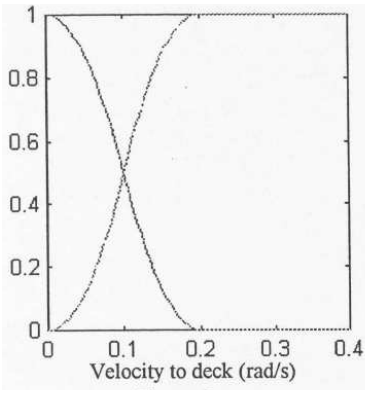

Fig. 9. Input membership functions: Inference system 1.

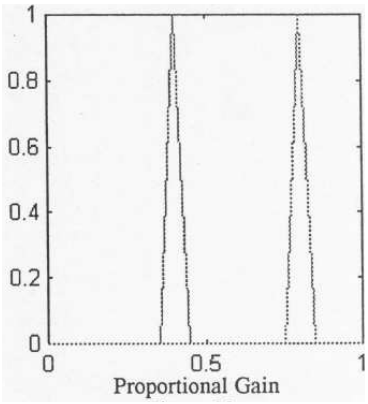

Fig. 10. Output membership functions: Inference system 1.

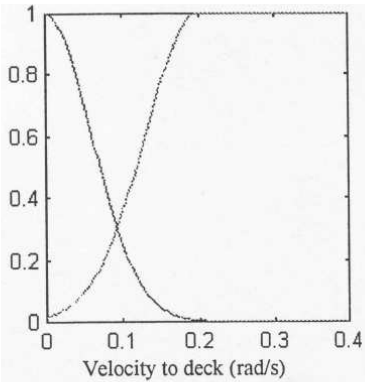

Fig. 11. Input membership functions: Inference system 2.

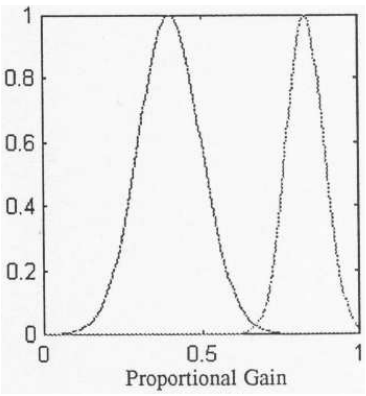

Fig. 12. Output membership functions: Inference system 2.

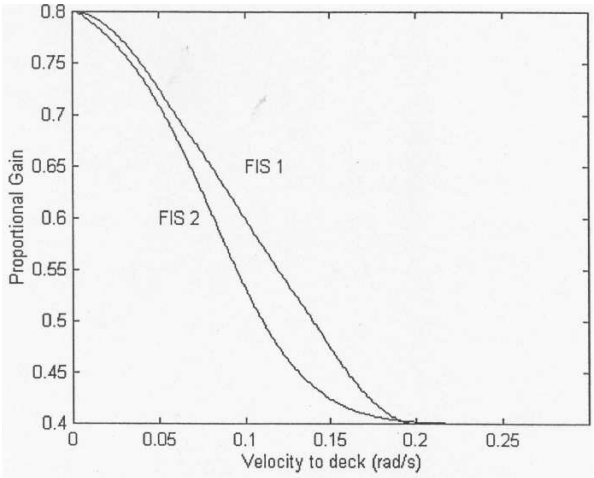

Fig. 13. Resultant mappings produced by fuzzy engines for the proportional gain.

Two different t-norms for interpretation of fuzzy implication were also considered, leading to the 'min', or 'minimum', operation rule and the 'prod', or 'product', operation rule of the fuzzy implication. The mappings produced utilising either process are very similar, and this is shown in Fig. 15. This graph shows the relation be-

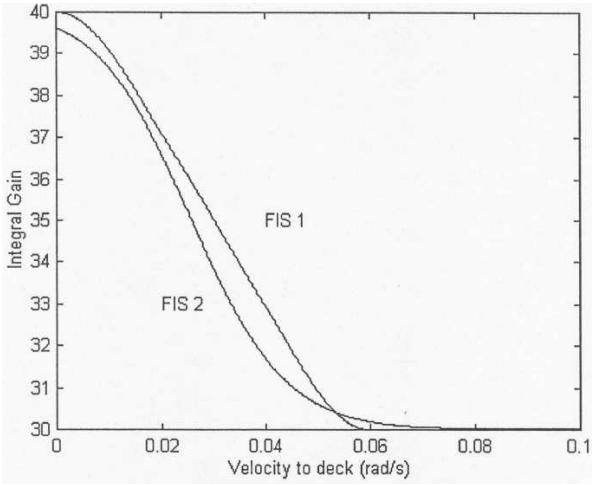

Fig. 14. Resultant mappings produced by fuzzy engines for the integral gain.

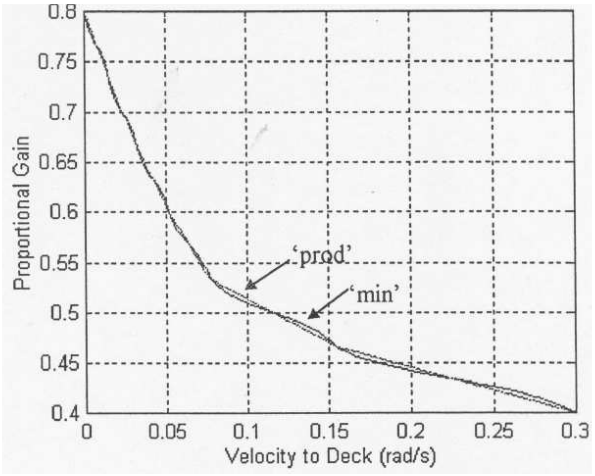

Fig. 15. Effect of the implication method on scheduling functions.

tween the velocity and the proportional gain for a fuzzy system employing seven triangular membership functions on the input and the output for both the different implication methods considered. The 'prod' curve is made up of a series of straight lines and the 'min' curve is made up of a series of shallow 's'-shaped bends. Clearly, there is little to choose between the two alternatives. It was found that the 'min' method gave slightly better performance and it was therefore this method that was used throughout the simulation work.

Integral Gain Scheduling

It was found that the best tracking performance was given using integral scheduling functions of the same shape as their proportional gain counterparts, but over a different range. The integral gain can be varied at a greater rate than the proportional gain before instability occurs. Figure 14 shows the input-output relations for the integral gain scheduling functions; the membership functions used to generate these mappings are identical to those described for the proportional gain, but over different ranges.

4.3. Multiple Input Scheduling System

Consideration was also given to the possible improvements that might be available by incorporating another input into the fuzzy logic inference system. The specific motivation for this was that the reduction of the transient error spikes at the end of the ship roll increased the overshoot in the position response. This is obviously undesirable. It was thought that the use of a predictive component in the scheduling functions would make the controller capable of responding to the servo coming out of stiction much more rapidly than by observing the velocity in isolation. This predictive component could be the derivative of the velocity signal or possibly the derivative of the error signal. The problems with this approach are twofold. Firstly, obtaining the derivative of the signals is difficult since they are heavily contaminated with noise and therefore cannot be differentiated as they are. The use of a filter is imperative but also poses problems, since any filter capable of reducing the noise to a differentiable level is likely to also filter out the very dynamics which would be of use. This is demonstrated in Fig. 16, which shows the filtered and then differentiated velocity to deck for a zero reference input to the outer loop (the ERT situation). For the first case the velocity to deck is filtered by a second-order Butterworth filter with a cut-off frequency of 3 Hz. The noise level has been reduced sufficiently to enable differentiation, but the dynamics at the stiction points (5 and 10 seconds) are barely noticeable. Increasing the cut-off frequency of the filter makes the stiction dynamics more pronounced, but the differentiated signal becomes

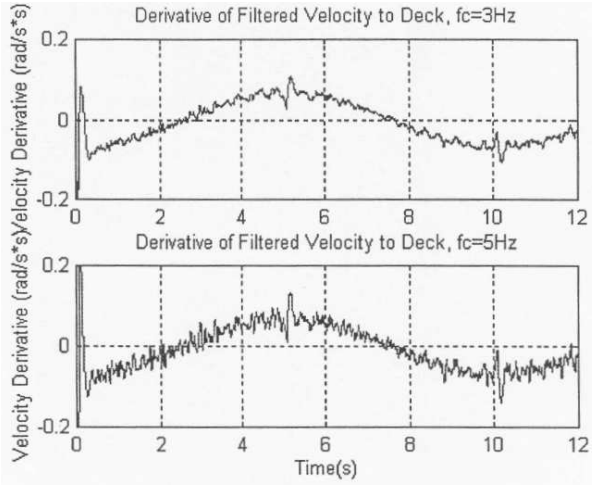

Fig. 16. Filtered and differentiated velocity to deck.

too noisy—this is also shown in Fig. 16. The other problem is that using a predictive element might vary the controller parameters too rapidly for the system and cause instability.

So far investigations into using multiple input fuzzy inference systems have not produced any valuable results due to the two problems mentioned above. Fuzzy engines have been developed using the velocity derivative and the error derivative in conjunction with the velocity to deck signal, and the mappings are shown in Figs. 17 and 18. As yet the difficulties in obtaining the respective derivative signals have meant that the multiple input inference systems have remained untried in the simulation model.

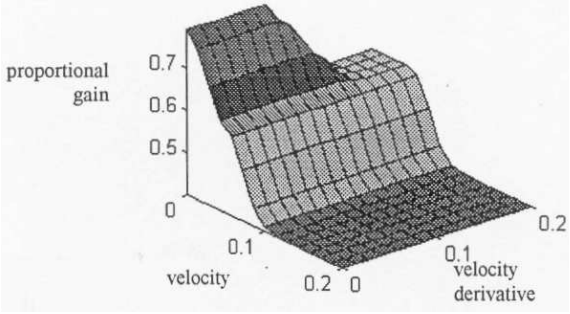

Fig. 17. Scheduling function control surface using the velocity and the derivative.

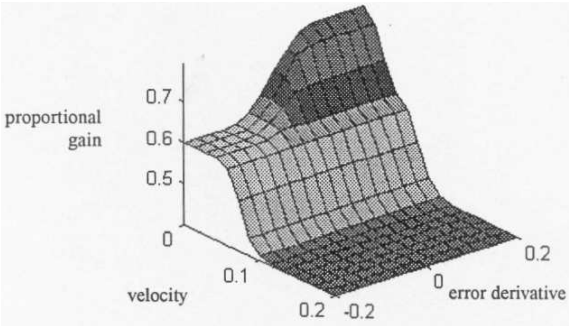

Fig. 18. Scheduling function control surface using the velocity and the error derivative.

5. Outer Loop Controller Design

A non-linear controller was designed for the inner loop to compensate for the non-linearities in the plant model. The controller in the outer loop does not have to deal with any non-linearities directly, so standard linear control methodologies can be applied. For simplicity, a PID controller was used:

$$PID(s) = K\left(\frac{s+T_i}{s} + Ds\right), \tag{16}$$

where D is the derivative gain, T_i stands for the integral gain and K is the proportional gain.

A numerical optimisation routine was employed in the outer loop to find the 'best' controller parameters (proportional, integral and derivative gains) in terms of minimising the position error in the outer loop response. Two different scenarios were considered—the end-of-roll transient case (a zero reference input to the outer loop) and a more 'standard' tracking profile for an airborne target corresponding to a target moving on a straight line with a fixed linear velocity a fixed height above sea level. The angular position and velocity profiles associated with this second tracking scenario are shown in Fig. 19, where the target is moving at a constant velocity of 300 m/s at a height of 300 m above sea. The shortest distance in a horizontal plane from the tracker to the target is also 300 m.

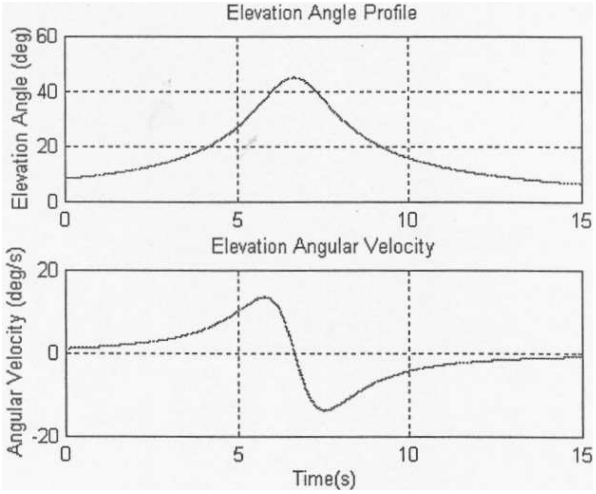

Fig. 19. Tracking profiles.

Different situations were examined because different parameters were likely to be optimum for different tracking situations. Optimisation results can only be used as a guide for the controller gains since some consideration also has to be given to robustness, and a compromise has to be made between optimum values for the different tracking circumstances. The controller parameters were found that minimised the total of the error squared, so the 'cost function' can be written as

$$C = \int e^2(t)\,\mathrm{d}t. \tag{17}$$

The proportional gain was fixed at a value of five to reduce the procedure to a two-degree-of-freedom optimisation and hence to save the computation time. Limiting the proportional gain also gives some insurance against instability. With more time a full three-degree-of-freedom optimisation could be carried out for both tracking profiles mentioned. The optimisation results showed that using a

large derivative term in the outer loop controller dramatically reduces the transient error for low velocity tracking (due to its predictive nature). A lower derivative gain, however, is preferable for high velocity tracking. The optimum integral gain was similar for both tracing scenarios. Some of the relevant simulation results are shown in Section 6. Some compromise has to be made between the high derivative term required to minimise the end-of-roll transient error and a lower (or non existent) derivative gain which gives better tracking performance at higher velocities. Simulations have shown that a linear PID controller with the transfer function of

$$PID(s) = 5\left(\frac{s+2.5}{s} + 0.1s\right) \tag{18}$$

provides enough reduction in the transient error (within the specification limits) while still performing well out of stiction and providing the necessary robustness.

6. Simulation Results

6.1. Results for Inner Loop Controller Design

Two different simulation results are presented here, showing the response of the servo system to a zero reference input to the position loop. In Fig. 20 the inner loop controller has proportional gains scheduled by the 'FIS 1' shown in Fig. 13, and the integral gain is varied by the 'FIS 1' which produces the mapping shown in Fig. 14. The second simulation response that is illustrated in Fig. 21 utilises the other type of fuzzy inference engine (FIS 2) described in Section 4 for both the controller parameters. In both the cases the outer loop controller was a fixed linear controller of PI type with the transfer function (14).

Comparing these two results with the zero reference response of the system incorporating a fired linear controller in the inner loop (Fig. 7), it can be seen that the error spikes at the end-of-roll time instants have been considerably reduced, so that the low velocity tracking specification has been met. In terms of the total error, the fuzzy engine using Gaussian membership functions performs better than the alternative previously discussed. Using this fuzzy inference system, the variation in the PI controller parameters during the end-of-roll transient scenario is shown in Fig. 22. This figure shows that the proportional gain is varying at a much slower rate than the integral gain.

Some effort was made to find the optimum parameters of the membership functions which make up the fuzzy inference systems described here. The completion of a full numerical optimisation routine is a fairly complex problem. Firstly, some sort of stability analysis has to be performed on the inner loop to give the stability boundaries

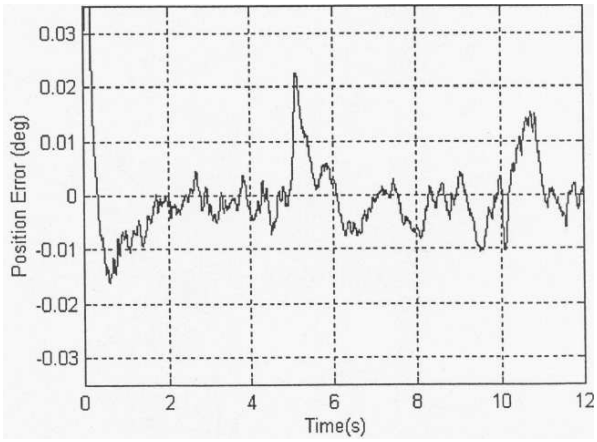

Fig. 20. Response using FIS 1 for controller parameters.

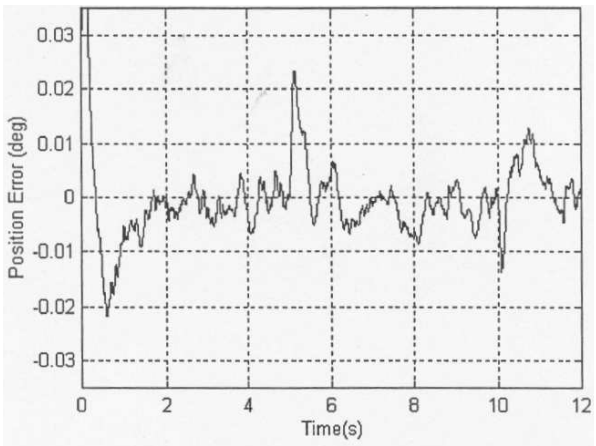

Fig. 21. Response using FIS 2 for controller parameters.

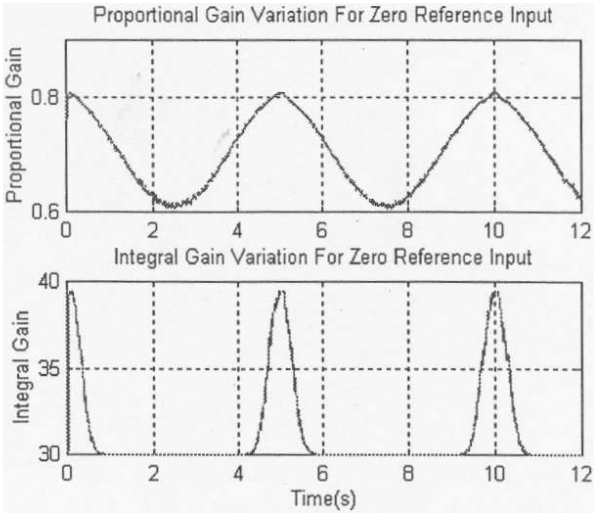

Fig. 22. Controller parameter variations.

on the membership function parameters. Then the optimisation routine itself will require a significant amount of computation time. If, for example, a fuzzy inference sys-

tem with two Gaussian membership functions on the input and output was used to schedule both the proportional and integral gains, then the optimisation has sixteen degrees of freedom (two inference systems, each with two membership functions on the input and output with each membership function being specified by two parameters (mean and standard deviation for Gaussian functions)).

6.2. Results for Outer Loop Controller Design

Figure 23 shows the response of the servo system to a zero reference input when the inner loop controller is a fuzzy logic gain scheduled controller (using FIS 2) and the outer loop controller is a linear PID controller with a large derivative term ($D = 0.4,\ K = 5,\ T_i = 2$). Comparing this response with that of Fig. 21, which is the same situation but with no derivative term in the outer loop controller, it can be seen that the transient error spikes have been further reduced. Figure 24 then shows the effect

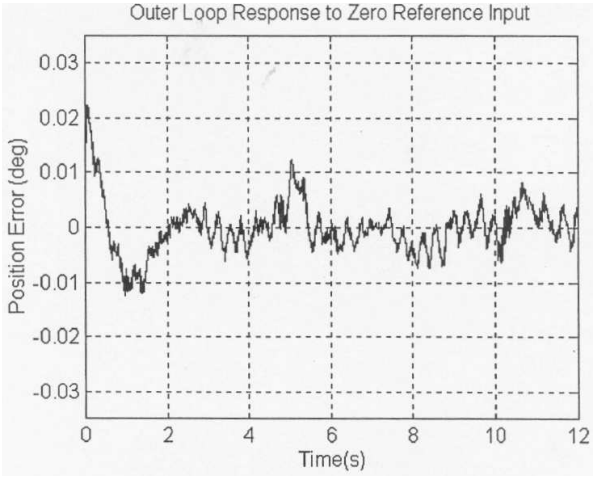

Fig. 23. Reduction in the transient error using the derivative term.

of the derivative term on higher velocity tracking. The response of the system to the tracking profile detailed in Fig. 19 is pictured. From the two profiles in Fig. 24 it is obvious that the response with the higher derivative term gives a greater tracking error.

7. Conclusions

This paper has discussed the application of gain scheduled control to a real-life servo control problem. Fuzzy logic has been used in a supervisory role to provide the scheduling algorithms. It has been shown that this method can be used to compensate for the hard non-linearities found in such control applications. For the particular case studied here the use of fuzzy logic gain scheduling applied to the inner-loop controller meant that the specifications for

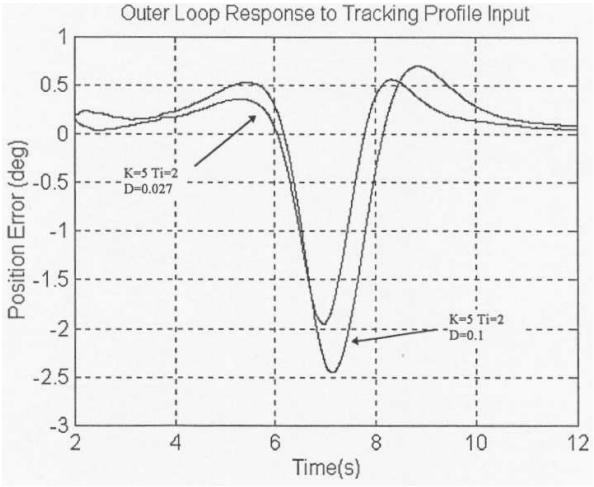

Fig. 24. Effect of the derivative term on high velocity tracking.

low velocity tracking could be met with a stable closed loop control system. This was not achievable with a linear controller in the inner loop. Further theoretical work is required on the stability of the closed inner loop in order to place limits on the membership function parameters of the fuzzy system, guaranteeing the closed loop stability of the inner velocity loop. This would allow complete numerical optimisation to be carried out on the fuzzy system. The success achieved here by applying this technique suggests that it is a possible solution for many servo control problems where the dynamics contain hard non-linearities such as stiction.

References

Brdyś M.A. and Sim W.L. (1995): *Fuzzy logic supervision of adaptive generalised predictive control of induction motor*. — Proc. 6-th Europ. Conf. *Power Electronics and Applications*, Sevilla, Spain, Vol. 3, pp. 3586–3591.

Brdyś M.A., Quevedo J. and Sim W.L. (1995): *Fuzzy logic supervisory control of induction motor under full range of operating conditions*. — Proc. 5-th Congress ESTLF'95, Murcia, Spain, pp. 185–191.

Canudas de Wit C. and Lichinsky P. (1997): *Adaptive friction compensation with partially known dynamic friction model*. — Int. J. Adapt. Contr. Signal Process., Vol. 11, No. 4, pp. 65–80.

Canudas de Wit C., Olsson H., Astrom K.J. and Lichinsky (1995): *A new model for control of systems with friction*. — IEEE Trans. Automat. Contr., Vol. 40, No. 3, pp. 419–425.

Garnell P. and East D.J. (1997): *Guided Weapon Control Systems*. — New York: Pergamon Press.

Hunt K.J. and Johansen T.A. (1997): *Design and analysis of gain-scheduled local controller networks*. — Int. J. Contr., Vol. 66, No. 6, pp. 619–651.

Lichinsky C., Canudas de Wit C. and Morel G. (1999): *Friction compensation for an industrial hydraulic robot*. — IEEE Trans. Contr. Syst. Mag. Vol. 19, No. 1, pp. 25–32.

Passino K.M. and Yurkovich S. (1998): *Fuzzy Control*. — Menlo Park, California: Addison-Wesley.

Shamma J.S. and Athans M. (1990): *Analysis of gain scheduled control for non-linear plants*. — IEEE Trans. Automat. Contr., Vol. 35, No. 8, pp. 897–907.

Singer R.A. and Behnke K.W. (1970): *Real-time tracking filter evaluation and selection for tactical applications*. — IEEE Trans. Aerospace Electr. Syst., Vol. 7, No. 1, pp. 100–110.

Wang Li-Xin (1994): *Adaptive Fuzzy Systems And Control: Design and Stability Analysis*. — Englewood Cliffs: Prentice Hall.

Received: 12 February 2001
Revised: 17 July 2001
Re-revised: 10 October 2001